BOLLETTINO DI GEOFISICA TEORICA ED APPLICATA VOL. XXXV, N. 140 - DECEMBER 1993

E. E. PAPADIMITRIOU

# FOCAL MECHANISM ALONG THE CONVEX SIDE OF THE HELLENIC ARC

**Abstract.** The focal mechanisms of eleven large earthquakes that have occurred during recent decades in the Hellenic Arc are determined. For each earthquake the long-period P and SH waveforms were inverted to estimate the parameters of the best fitting point source, including seismic moment, centroid depth, double-couple source orientation, and source time function. Four of these earthquakes occurred in the northwestern end of the Hellenic Arc and have strike-slip faulting mechanisms with fault planes striking SW-NE. Three other earthquakes from the area of Zakynthos, and four near the Crete island, that is along the Hellenic Arc, are characterized by thrust faulting. Reliable fault plane solutions, already published, are also taken into consideration in order to examine the motion taking place along the whole Arc, using all the available data. The whole data set was separated into four groups, and for each one, the representative fault plane solution determined. It is found that the direction of the maximum compression axis P changes from ENE to NNE going from west to east along the Arc.

## INTRODUCTION

The Aegean region is an area of intense seismic activity compared to surrounding regions, and one in which seismological and geological evidence indicate a very complex and rapidly varying tectonic picture. Its most characteristic feature is the Hellenic Arc, which lies in its southern part. The study of this arc is of great interest, since it is located along the convergent boundary of the Eurasian and African lithospheric plates. Plate convergence is accomodated by northward subduction of the African lithosphere beneath the Eurasian plate along the Hellenic Trench (Papazachos and Comninakis, 1969, 1971).

The knowledge of the tectonic properties of island-Arc systems is of great interest since it contributes to the solution of a variety of important problems, some of which are of practical interest. The source characteristics of earthquakes in such regions provide adequate information for this scope. It is in this context that the source characteristics of large earthquakes along the Hellenic Arc are studied. Several studies have been performed on the seismotectonics of this area, based on fault plane solutions from both P wave onsets and waveform modelling (McKenzie, 1972, 1978; Scordilis et al., 1985; Papazachos et al., 1984, 1986, 1991; Anderson and Jackson, 1987; Bezzeghoud, 1987; Papadimitriou, 1988; Kiratzi and Langston, 1989, 1991; Ioannidou, 1989; Beisser et al., 1990; Taymaz et al., 1990; Liakopoulou et al., 1991). In many respects, these studies corroborate each other, but many uncertainties in the interpretation remain. It is the purpose of this study to investigate in detail the focal mechanisms and source parameters of events in the Hellenic Arc in order to obtain a clearer picture of the type of faulting taking place there. Hence, after a brief review of the regional plate tectonic framework, and presentation of both the data and analysis, the results of the study are discussed



Manuscript received, December 29, 1992; accepted, October 15, 1993.

Laboratory of Geophysics, University of Thessaloniki, Thessaloniki GR54006, Greece.

in relation to current understanding of the relative motion between the African and Eurasian plates in the vicinity of the Hellenic Arc.

## SEISMOTECTONIC SETTING

The Aegean Arc is an active part of the Alpine-Himalayan belt, which forms one of the continental fracture systems of the earth. It lies between the Adriatic continental collision in the NW and the Arabic continental collision to the east. The seismic activity is very high throughout the arc, due to the subduction of the African lithospheric plate under the Aegean. The whole region is dominated by thrust faulting, with the direction of the axis of maximum compression NE-SW.

Fig. 1 illustrates the main seismotectonic features of the Aegean and surrounding areas (Papazachos et al., 1991). North of Cephalonia, on Lefkas island, the belt of thrust faulting, which runs along southwestern coastal Jugoslavia and continues south along the coastal regions of Albania and northwestern Greece, terminates. This type of faulting is connected with the continental collision between the Outer Hellenides and the Apulian microplate. The direction of the maximum compression axis is almost normal to the direction of the Adriatico-Ionian geological zone.

In the northernmost part of the arc, on Cephalonia island, dextral strike-slip faulting is observed, in agreement with the known relative motion of the Aegean and eastern Mediterranean. The existence of a transform fault has been suggested by Finetti (1976) in order to explain the connection of the compressional zone of the Hellenic Arc with the compressional zone of the eastern boundary of the Apulian lithospheric plate. McKenzie (1978), on the basis of both small-scale bathymetry (Stride et al., 1977) and geological mapping on land (British Petroleum, 1971), suggested that, at the northwestern end of the Arc, the deformation is taken up by a number of right-handed strike-slip faults which connect the deformation of northwestern Greece to the Hellenic Arc. According to Dewey and Sengor (1979) a right-lateral transform fault between Cephalonia and Zakynthos is suggested by the northward termination of the Hellenic Trench and an offset in seismicity.

In the southern part of the Aegean area, that is, from Cephalonia to Rhodos island, both shallow and intermediate depth seismic activity takes place. Papazachos and Comninakis (1969, 1971) found that the intermediate depth earthquakes in the region of Greece lie close to an amphitheatre-like surface, which is dipping under the arc at a mean angle of about 30°. The main belt of the shallow shocks is located in the outer part of the arc but on the landward side of the Hellenic Trench. They gave the general features of the arc from the concave to the convex side as follows: an inner igneous part, which includes volcanoes active in historic times, and which is underlain by intermediate earthquakes of a mean of 150 km focal depth; a shallow trough with maximum water depth of about 2000 meters; a zone of intermediate earthquakes with a focal depth equal to 100 km; a sedimentary arc consisting of mountains or islands; a zone of shallow earthquakes or intermediate earthquakes with focal depths smaller than 80 km; the Hellenic Trench with maximum water depth equal to about 5000 meters; and a zone of shallow shocks.

A back-arc basin, the Aegean Sea with its active volcanoes, extends landwards. Its broad tectonic framework is dominated, as shown by McKenzie (1972), by the rapid westward motion of the Anatolian plate relative to the Black Sea, and the west-southwestward motion of the Aegean area relative to the Eurasian plate. The type of faulting, based on the most reliable fault plane solutions, shows a clear N-S extension (Papazachos et al., 1991).

## DATA ANALYSIS AND INVERSION PROCEDURE

Long- and short-period P and SH World Wide Standardized Seismograph Network (WWSSN) seismograms recorded at teleseismic distances are inverted simultaneously to determine the centroid depth, far-field source time function, seismic moment, and source mechanism (strike,

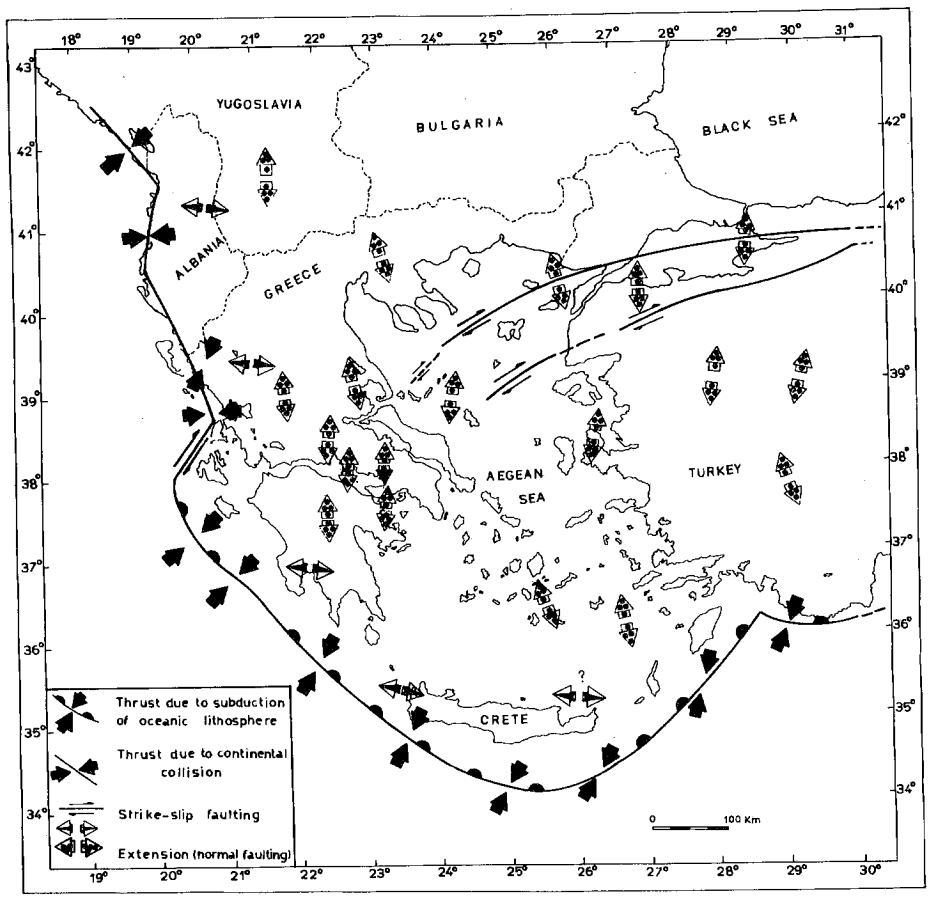


Fig. 1 — A graphic presentation of the stress pattern of the Aegean and the surrounding area (after Papazachos et al., 1991).

dip and rake) using the inversion technique of Nabelek (1984). To avoid the strong effects of the upper mantle and the core, the stations are limited to the epicentral distance range of 30° to 90° for P waves, and 30° to 70° for SH waves. The data are hand-digitized and interpolated at four and two samples per second for P and S waves, respectively. Both N-S and E-W components of the S-waves are rotated to produce SH waves. The seismograms are equalized to a common instrument magnification and epicentral distance, and are weighted in the inversion to equalize any bias in the azimuthal distribution of the data (Nabelek, 1985). In cases where the P waveforms display only compressional first motions, the SH seismograms are weighted analogously in order to contribute more to a well constrained solution. The onset of the P arrival for each record is determined, when possible, from short-period seismograms.

The earthquake source parameters are estimated by matching the observed seismograms with the theoretical ones in a least-squares sense using procedures discussed by Nabelek (1984, 1985). The source is approximated by a point source with a double-couple mechanism, scalar seismic moment and far-field time function (moment-rate release as a function of time). The synthetic seismograms include the complete crustal response, but the most critical contribution to the centroid depth determination comes from the direct phases and the reflections from the free surface. Although there is some trade-off between the source depth and the time function in fitting the observed seismogram at a particular station, use of many stations distributed over a large azimuthal range reduces this trade-off significantly.

As far as the determination of the events located in the Ionian islands is concerned, the

**Table 1 — Epicentral data and source parameters of the earthquakes analyzed in the present study.**

| Date | Origin Time h: m: s | Epicentral coordinates φ°N | λ°E | $M_s$ | Depth (km) | Moment (*$10^{24}$ dyn cm) | Dur. (sec) | Strike | Dip | Rake |
|---|---|---|---|---|---|---|---|---|---|---|
| Nov. 15, 1959 | 17:08:43 | 37.8 | 20.5 | 6.8 | 12 | 171.8 | 14 | 46 | 37 | 187 |
| Dec. 16, 1963 | 13:47:53 | 37.0 | 21.0 | 5.9 | 7 | 1.3 | 2 | 296 | 16 | 101 |
| Jul. 08, 1969 | 08:09:13 | 37.5 | 20.3 | 5.9 | 12 | 3.8 | 5 | 353 | 18 | 116 |
| Sep. 17, 1972 | 14:07:15 | 38.3 | 20.3 | 6.3 | 8 | 21.6 | 8 | 45 | 68 | 186 |
| Nov. 29, 1973 | 10:57:44 | 35.2 | 23.8 | 6.0 | 18 | 4.2 | 5 | 283 | 38 | 97 |
| May 11, 1976 | 16:59:45 | 37.4 | 20.4 | 6.5 | 16 | 35.7 | 8 | 335 | 14 | 106 |
| Sep. 11, 1977 | 23:19:19 | 34.9 | 23.0 | 6.3 | 16 | 5.3 | 3 | 295 | 40 | 95 |
| Aug. 17, 1982 | 22:22:20 | 33.7 | 22.9 | 6.4 | 15 | 20.3 | 5 | 246 | 31 | 125 |
| Jan. 17, 1983 | 12:41:30 | 38.1 | 20.2 | 7.0 | 11 | 208.0 | 11 | 39 | 45 | 175 |
| Mar. 23, 1983 | 23:51:05 | 38.2 | 20.3 | 6.2 | 7 | 19.2 | 8 | 31 | 69 | 174 |
| Jun. 21, 1984 | 10:43:46 | 35.4 | 23.3 | 6.2 | 40 | 13.5 | 4 | 322 | 16 | 114 |

crustal structure around the source is assumed to be a half-space. The P- and S- wave velocities and the density of the half-space are assumed to be 6.5 km/s, 3.7km/s and 2.8 gr/cm$^3$, respectively. The half-space velocities are chosen so that they are approximately equal to the average velocity of the area, according to a model proposed by Panagiotopoulos and Papazachos (1985). For the events in the southern part of the Hellenic Arc, the crustal structure is assumed to be a top layer underlain by a half-space. The P- and S- wave velocities are assumed to be 6.0 km/s and 3.5 km/s, respectively, for the top layer, and 6.6 km/s and 3.8 km/s, respectively, for the half-space. The thickness of the top layer was taken to be 15 km and the density 2.8 gr/cm$^3$. These values are also consistent with the crustal model mentioned previously (Panagiotopoulos and Papazachos, 1985).

## RESULTS OF WAVEFORM INVERSION

The results obtained by body waveform inversion for the eleven events, using the computer program of McCaffrey and Abers (1988), are presented in Table 1. The double-couple mechanism is specified by three angles in the order strike, dip, and rake, using the convention of Aki and Richards (1980). The observed (solid) and synthetic (dashed) long- and short- period seismograms for each event are shown in a series of figures. The P waves are shown in the upper, and the SH waves in the lower part. In the middle portion of each half of the figure, the nodal planes of the direct P, and the nodal surfaces of SH waves are shown on lower- hemisphere, equal-area projections. Near the focal spheres the amplitude scale for the corresponding waves are shown. The far-field source time function and the time scale for both the P and SH waves are shown in the middle of each figure. The events are discussed and presented below in chronological order of occurrence.

*November 15, 1959.* The epicenter of this earthquake is located just off the northwestern coast of Zakynthos island. In spite of the small number of records available to us, due to the limited number of stations operating in that period, an adequate azimuthal coverage is obtained. Certainly, the nodal arrivals of the stations PAL and WAY seem crucial to constrain the NW-SE trending plane (Fig. 2). The overall matching gives a strike slip faulting (46/37/187) with a small normal component, and with a centroid depth of 12 km. The seismic moment is 1.7*10$^{26}$ dyn cm, and the duration of the source is about 14 s. McKenzie (1972) determined this mechanism as normal faulting, though he pointed out that it could well be thrust.

*December 16, 1963.* This earthquake occurred south of Zakynthos island. Anderson and Jackson (1987) reported a first-motion solution for this event as pure dip-slip thrust with an E-W strike for the fault plane. They pointed out that this mechanism is not easily compatible with any regional interpretation but, because it is clearly different from the other thrusting events to the north, may indicate motion on a transverse structure in the Hellenic Trench. North (1977), from surface-wave analysis, found that the seismic moment of this event equals to 4.8*10$^{24}$ dyn cm.

Both long- and short- period data have been used in determining the source parameters of this event. The best match occurs at a centroid depth of 7 km, with a thrust mechanism (296/16/101) and with the low angle nodal plane striking from WNW to ESE and dipping to the NE (Fig. 3). The seismic moment is $1.3*10^{24}$ dyn cm, considerably lower than that found from surface-wave analysis, and the duration of the source time function is about 2 s.

*July 8, 1969.* This event occurred southwest of Zakynthos island. From long-period P wave first-motion data, McKenzie (1972) gives a normal-faulting solution and noted that it could well be thrust. Anderson and Jackson (1987) suggest a pure dip-slip thrusting fault plane solution. The above solutions have an unconstrained very shallow dipping plane, and the steeper plane almost vertical. North (1977) estimated the moment as $4.1*10^{24}$ dyn cm from a surface wave analysis.

In spite of its small magnitude, this event is well recorded teleseismically. All the P waveforms have a clear compressional first motion; the small compressional first motions of the P waveforms at the stations NAI and AAE contribute to the constraint of the steep dipping plane (Fig. 4). The SH waveform data are well matched by the synthetic waveforms. The best fit to both P and SH observed waveforms is obtained with a centroid depth of 12 km and thrust-faulting mechanism (353/18/116) with the strike of the fault plane parallel to the axis of the Hellenic Arc in this region. The seismic moment is $3.8*10^{24}$ dyn cm, in good agreement with that found from surface wave data, and the duration of the source is about 5 s.

*September 17, 1972.* This event which occurred just off the west coast of Cephalonia is well recorded teleseismically. A good fit to the observed P and SH waveforms is obtained with a shallow centroid depth (8 km) and a strike slip - faulting mechanism (45/68/186) with a small normal component (Fig. 5) and with the strike of the SW dipping plane parallel to the local trend of the isobaths. The seismic moment is $2.2*10^{25}$ dyn cm, and the source has a duration of about 8 s. This focal mechanism was determined by McKenzie (1978) as a pure dip-slip thrust, with the use of P arrivals. Several additional first motions available led to a well constrained strike-slip solution by Anderson and Jackson (1987). The large number of both P and SH waveform data available to our study, which are well distributed in azimuth and generally well matched by the synthetic waveforms, ensure a strike-slip solution.

*November 29, 1973.* This earthquake occurred near the southwest coast of Crete. A good fit to the observed P and SH waveforms is obtained with a shallow centroid depth (18 km) and a thrust-faulting mechanism (283/38/97) with nodal planes oriented E-W (Fig. 6). The seismic moment is $8.0*10^{24}$ dyn cm and the source has a duration of about 5 s. The inversion solution reproduces the apparently compressional first motions of the P waveforms at all the stations which have high signal-to-noise ratios. The SH waveform data are well distributed in azimuth and are generally well matched by the synthetic waveforms, contributing to a well constrained solution.

Previous studies for the solution of the present earthquake are done by McKenzie (1978), Ioannidou (1989) and Taymaz et al. (1990). The solution given by McKenzie (1978) is quite similar to the solution suggested here, but with a very low angle fault plane (316/10/90).

*May 11, 1976.* The epicenter of this earthquake is located near to that of the July 8, 1969 event. From the many P wave records available for this earthquake, we selected the stations with highest signal-to-noise ratios. The P wave records are noisy due to the fact that they arrived over the signal, at the level of surface waves, of another earthquake which had occurred less than one hour before. A good fit to the observed P and SH waveforms is obtained with a predominantly thrust-faulting mechanism (335/14/106), a source time function of 8 s in duration, a centroid depth of 16 km, and a seismic moment of $3.6*10^{25}$ dyn cm (Fig. 7). The double-couple mechanism reported here is quite similar to that by Anderson and Jackson (1987) which was obtained from long-period P wave first-motion data, but our solution requires a steeper dip for the northeast dipping nodal plane, the strike of which is not well constrained both in their and our solutions. Taking into account that the Mediterranean sea floor is underthrusting the Hellenic mainland in this area in a NE direction, the fault plane can be taken with a NW strike, parallel to the axis of the subduction, without violating the match of the seismograms.

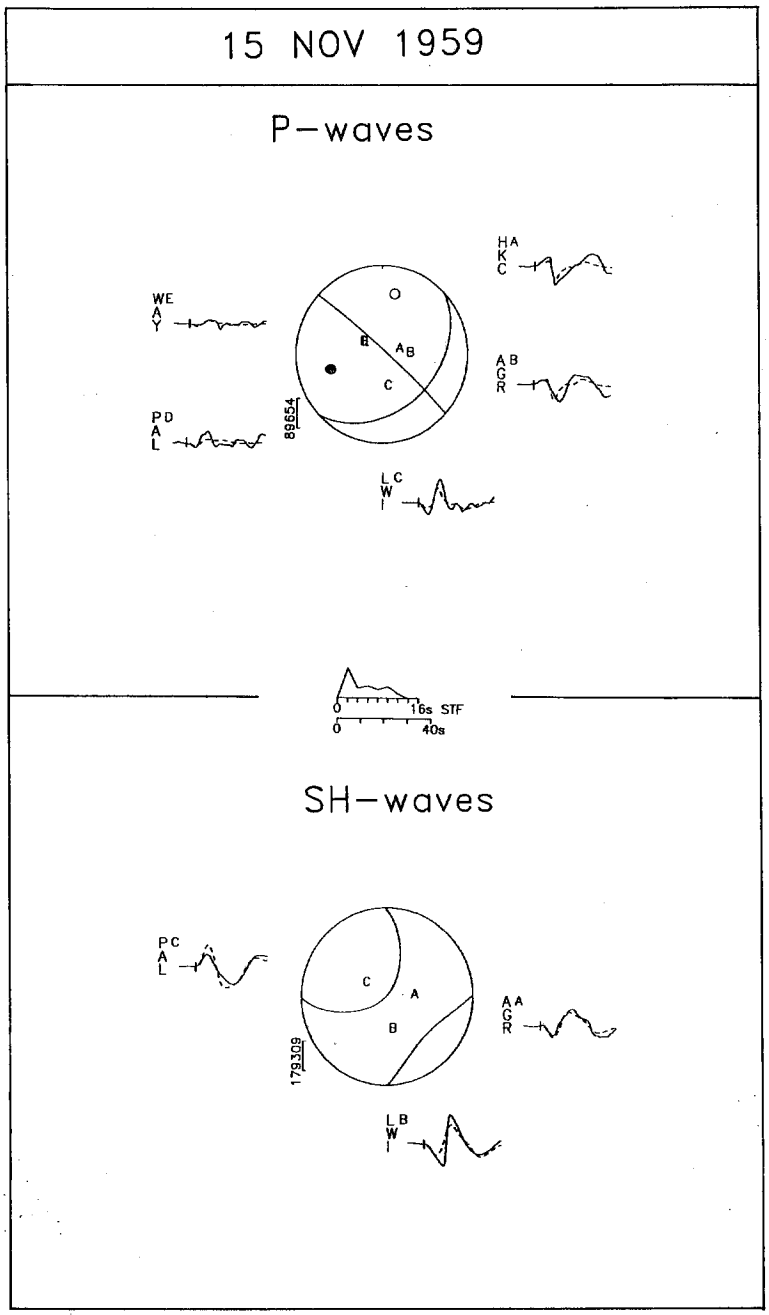


Fig. 2 — Observed (solid) and synthetic (dashed) long-period seismograms for the November 15, 1959 earthquake. P waves are shown on the top and SH waves on the bottom. In the middle portion of each half of the figure, the nodal planes of the direct P and SH waves are shown on lower-hemisphere, equal-area projections. Letters indicate the position of each station. Amplitude scales for both the P and SH waves are shown near the focal spheres. The far-field source-time function and the time scale are drawn in the middle of the figure.

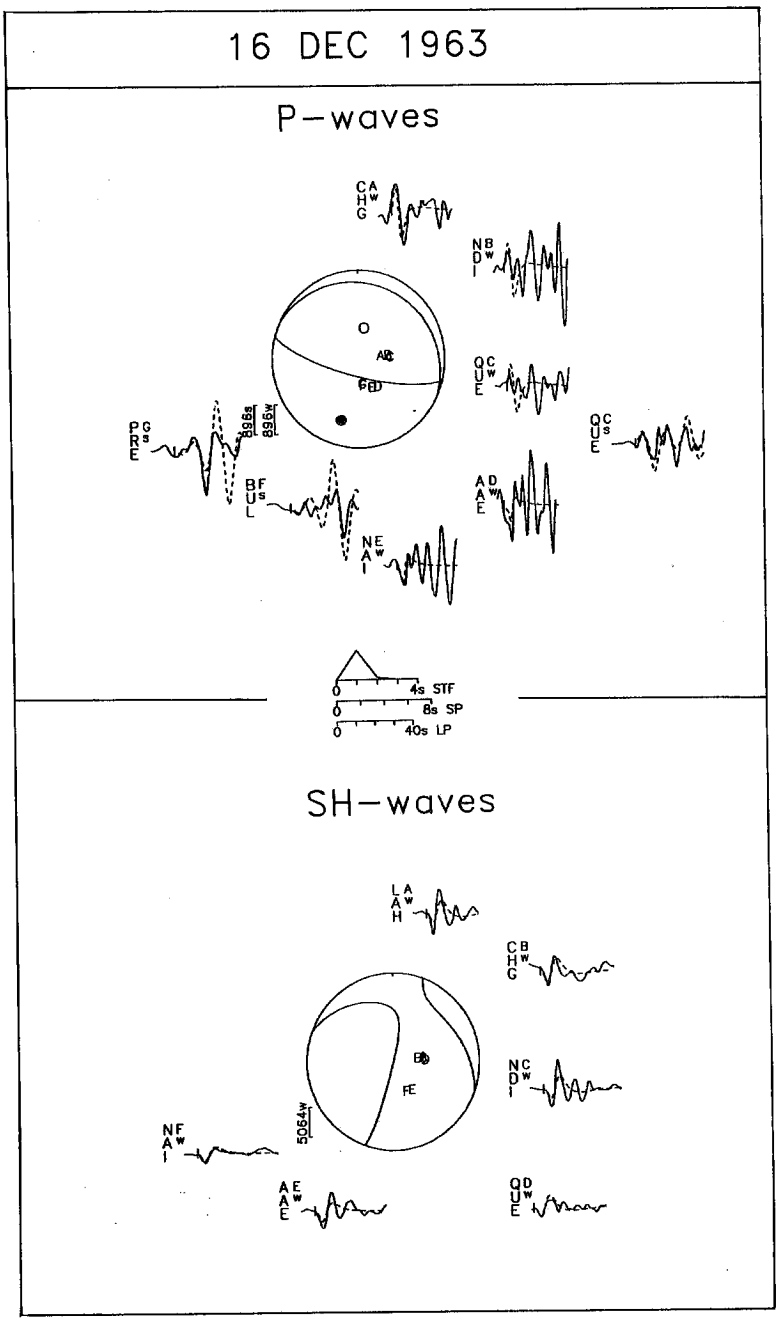


Fig. 3 — Observed (solid) and synthetic (dashed) long-period seismograms for the December 16, 1963 earthquake. All symbols are as described in Fig. 2.

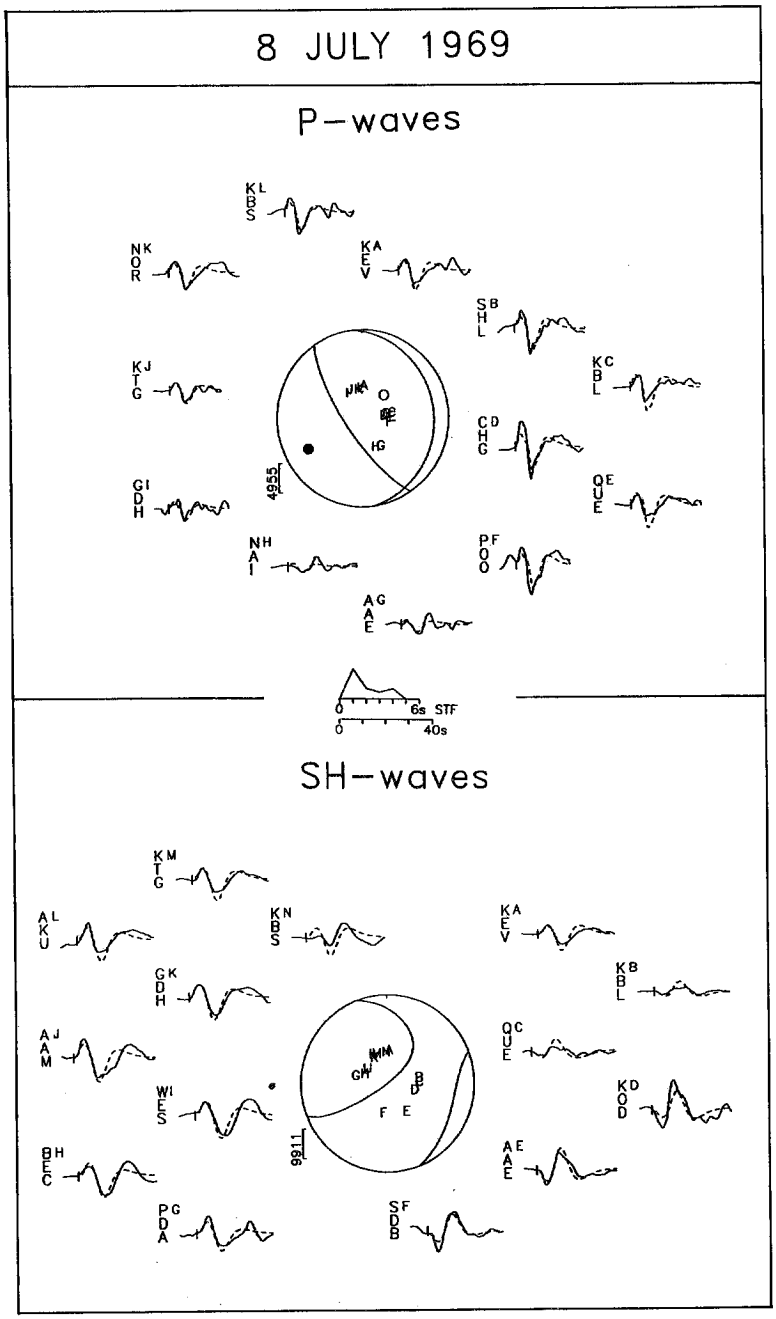


Fig. 4 — Observed (solid) and synthetic (dashed) long-period seismograms for the July 8, 1969 earthquake. All symbols are as decsribed in Fig. 2.

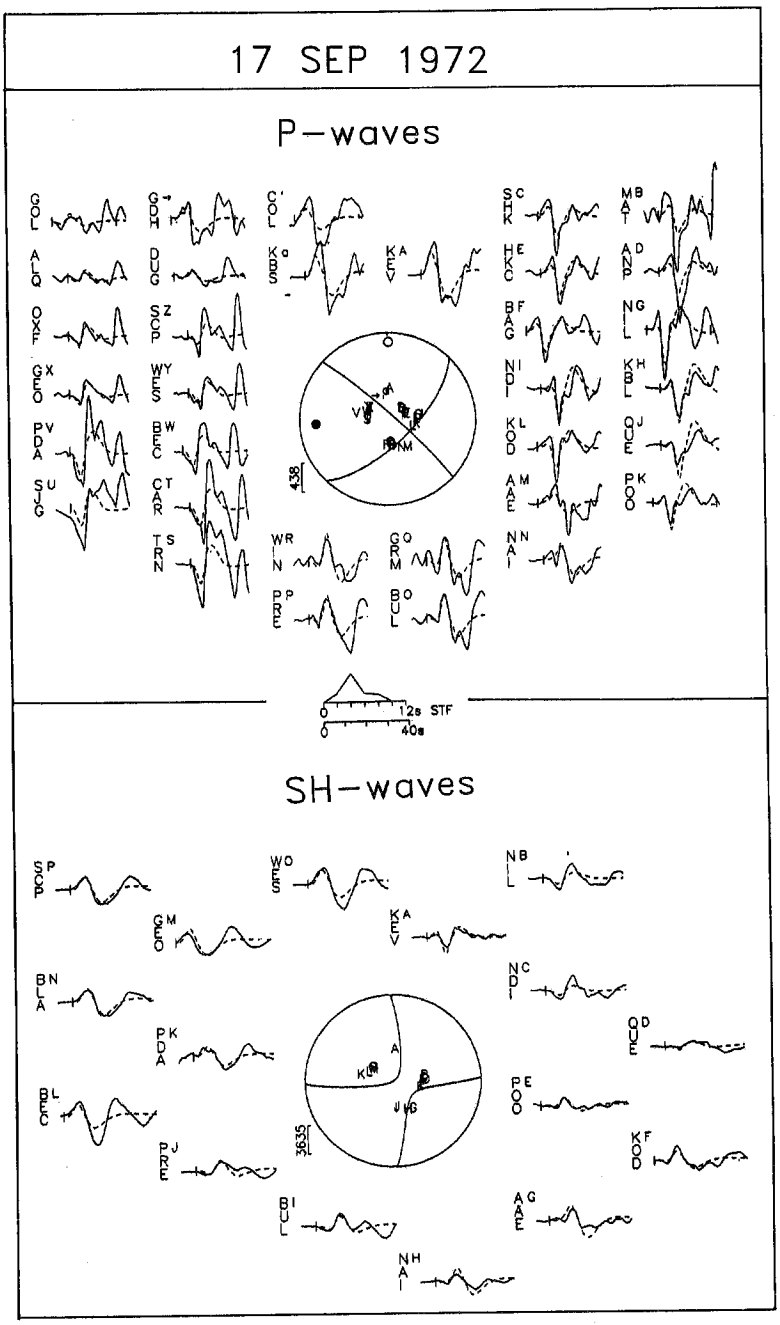


Fig. 5 — Observed (solid) and synthetic (dashed) long-period seismograms for the September 17, 1972 earthquake. All symbols are as described in Fig. 2.

*September 11, 1977.* The WNW-ESE trending nodal planes of this thrust faulting event are well constrained with many data available. This event occurred in the sea southwest of Crete. Station coverage is excellent for both P and SH waveforms (Fig. 8), and a good fit to the observed waveforms is obtained with a thrust faulting mechanism (295/40/95) with the lower angle nodal plane, which is considered as the fault plane, dipping to the north. The centroid depth of the best fitting solution is 16 km, the seismic moment is $5.3*10^{24}$ dyn cm, and the total duration of the rupture is about 3 s. All the P waveforms have a clear compressional first motion. Although the match of the synthetic to the observed waveforms is quite satisfactory, there are some inconsistencies in the amount of compression observed in the P waveforms recorded at stations near one another; SHI has as much as twice the compression as has the respective synthetic waveform, and much larger than the P waveforms recorded at stations KBL and KOD, for example. The good azimuthal coverage and matching of the synthetic to the observed SH waveforms contributed to a reliable solution. A similar solution is also suggested by Taymaz et al. (1990).

*August 17, 1982.* This earthquake occurred in the Mediterranean Ridge, about 150 km from the southwest coast of Crete. Station coverage is good for both the P and SH waveforms (Fig. 9). All the P waveforms display clear compressional first motions. An effort was then made to fit in amplitude the synthetic to the observed seismograms. The SH waveform data contribute more in fixing the solution, since they display both compressional and dilatational first motions and are excellently distributed in azimuth.

The best fit to the waveforms is obtained with a thrust faulting mechanism (246/31/125), with the fault plane oriented ENE-WSW and dipping to the NNW, at a depth of 15 km. The seismic moment is $20.3*10^{24}$ dyn cm and the total duration of the rupture is 5 s.. Taymaz et al. (1990) also suggested a thrust faulting for this event.

*January 17, 1983.* This is one of the largest earthquakes to have occurred in the area studied, and has been investigated by several scientists. Its epicenter lies SW of Cephalonia, in an area which had been characterized as a seismic gap (Papadimitriou and Papazachos, 1985) before its occurrence.

From long- and short- period P wave first motion data, Scordilis et al. (1985) were the first to suggest a right-lateral, strike-slip faulting with a small thrust component, and a fault striking in an approximately NE-SW direction. Their choice was supported by the epicentral distribution of a large number of aftershocks. Anderson and Jackson (1987), also working on P arrivals, noted that a strike-slip mechanism cannot easily be drawn for this earthquake, and suggested a pure dip- slip thrust. The Harvard centroid moment tensor (HMCT) solution is primarily a thrusting mechanism indicating a NE-SW compression (Dziewonski et al., 1983) and a depth of 10 km. Body wave modelling by Bezzeghoud (1987), Papadimitriou (1988), Ioannidou (1989), Kiratzi and Langston (1991) and Liakopoulou et al. (1991) support the strike slip solution.

An adequate number of P and SH wave data for this event, with good azimuthal coverage, are available to us. The good fit to the observed waveforms (Fig. 10) is obtained with a strike slip faulting mechanism and a small thrust component (39/45/175) at a centroid depth of 11 km. The seismic moment is $2.0*10^{26}$ dyn cm, and the duration of the source time function is about 11 s. The nodal arrivals at the stations to the west contributed in fixing the NW-SE trending plane, while the shallow dipping one is not so well constrained. The latter is considered in our solution as the fault plane, with its strike in quite good agreement with the bathymetric expressions and the orientation of the aftershock zone as derived by Scordilis et al. (1985).

*March 23, 1983.* The epicenter of this event lies very close to the epicenter of the previously presented event. This shock is the largest aftershock of the January 17, 1983 earthquake. In spite of the relatively noisy records, the adequate number of records available, and the good azimuthal coverage of the stations, clearly support a strike slip faulting mechanism with a small thrust component (31/69/174), very similar to that of the September 17, 1972 event (Fig. 11). The NE-SW trending nodal plane is fairly well constrained, with nodal P-arrivals certainly at stations SHL, CHG and NDI. Although the initial half-cycles for the stations NAI and CAR are slightly out of phase, the nodal SH arrivals at the stations DAG, KBS and KEV, however,

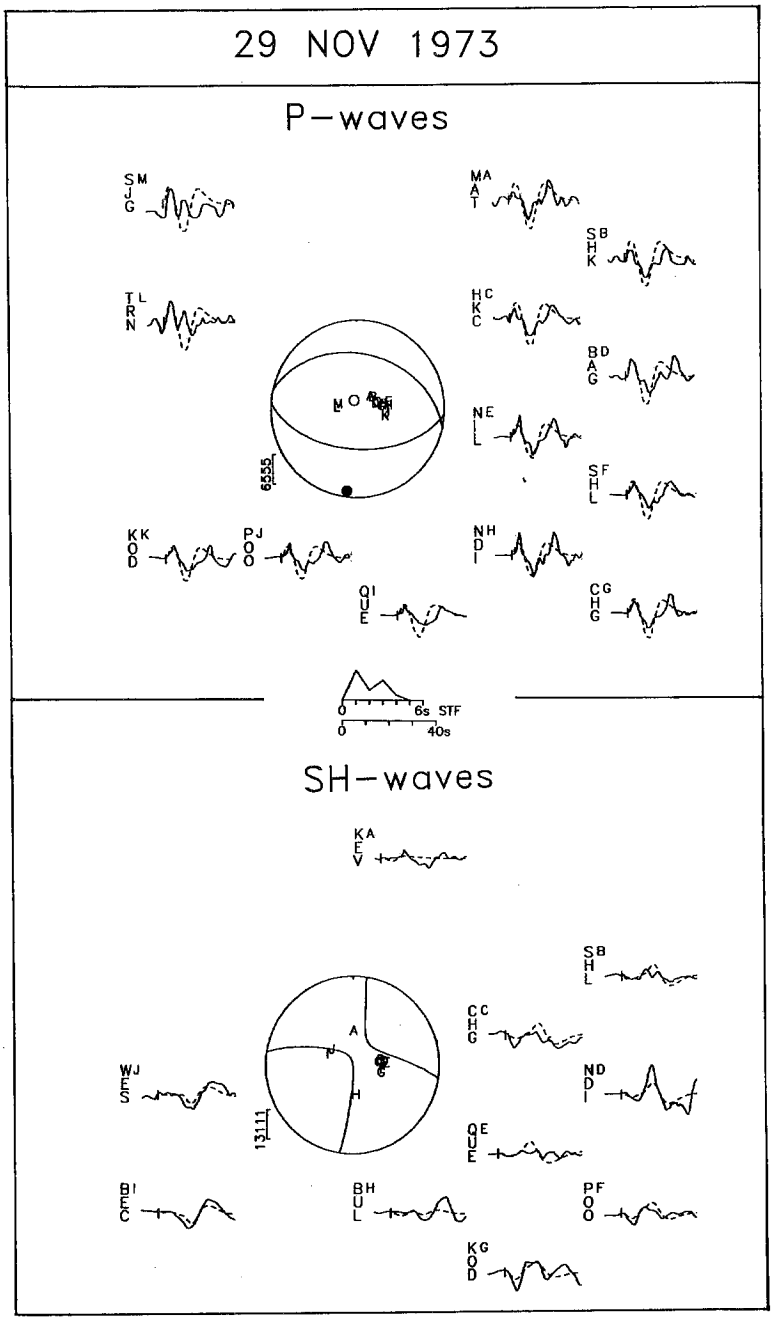


Fig. 6 — Observed (solid) and synthetic (dashed) long-period seismograms for the November 29, 1973 earthquake. All symbols are as decsribed in Fig. 2.

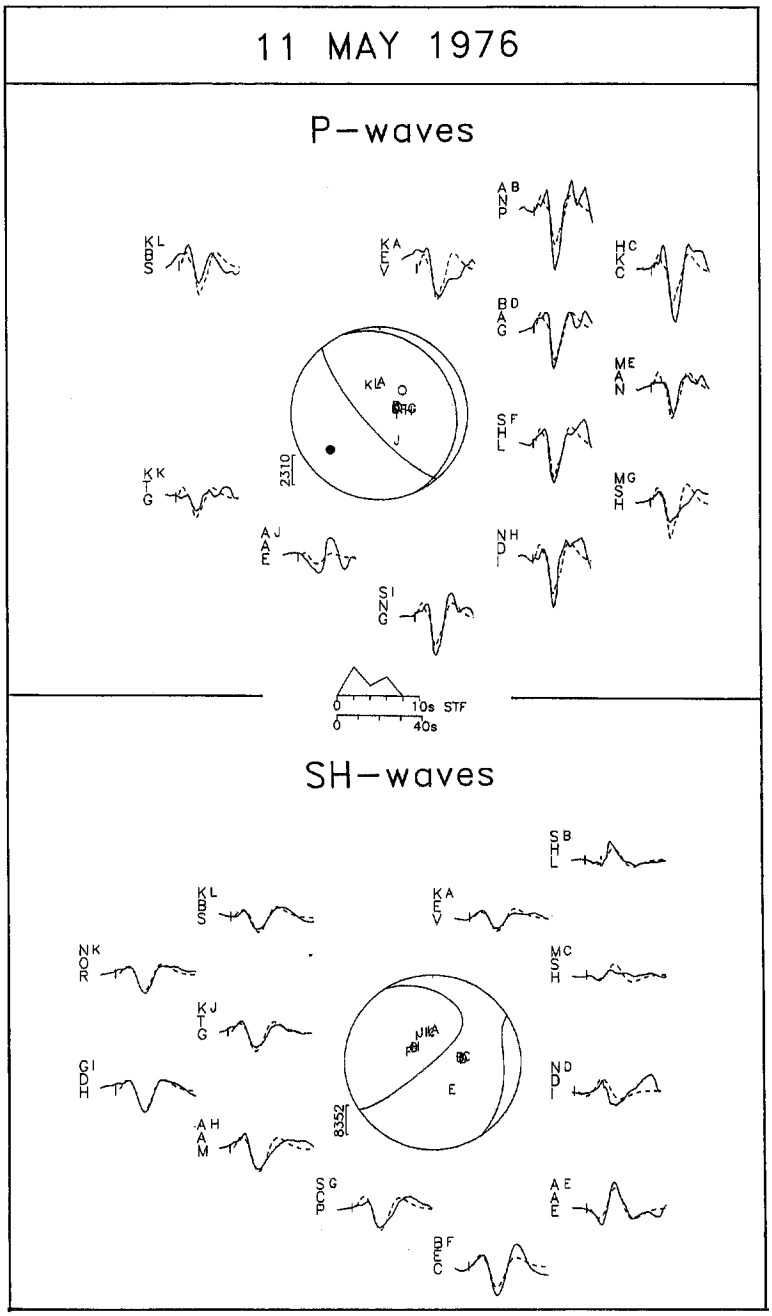


Fig. 7 — Observed (solid) and synthetic (dashed) long-period seismograms for the May 11, 1976 earthquake. All symbols are as described in Fig. 2.

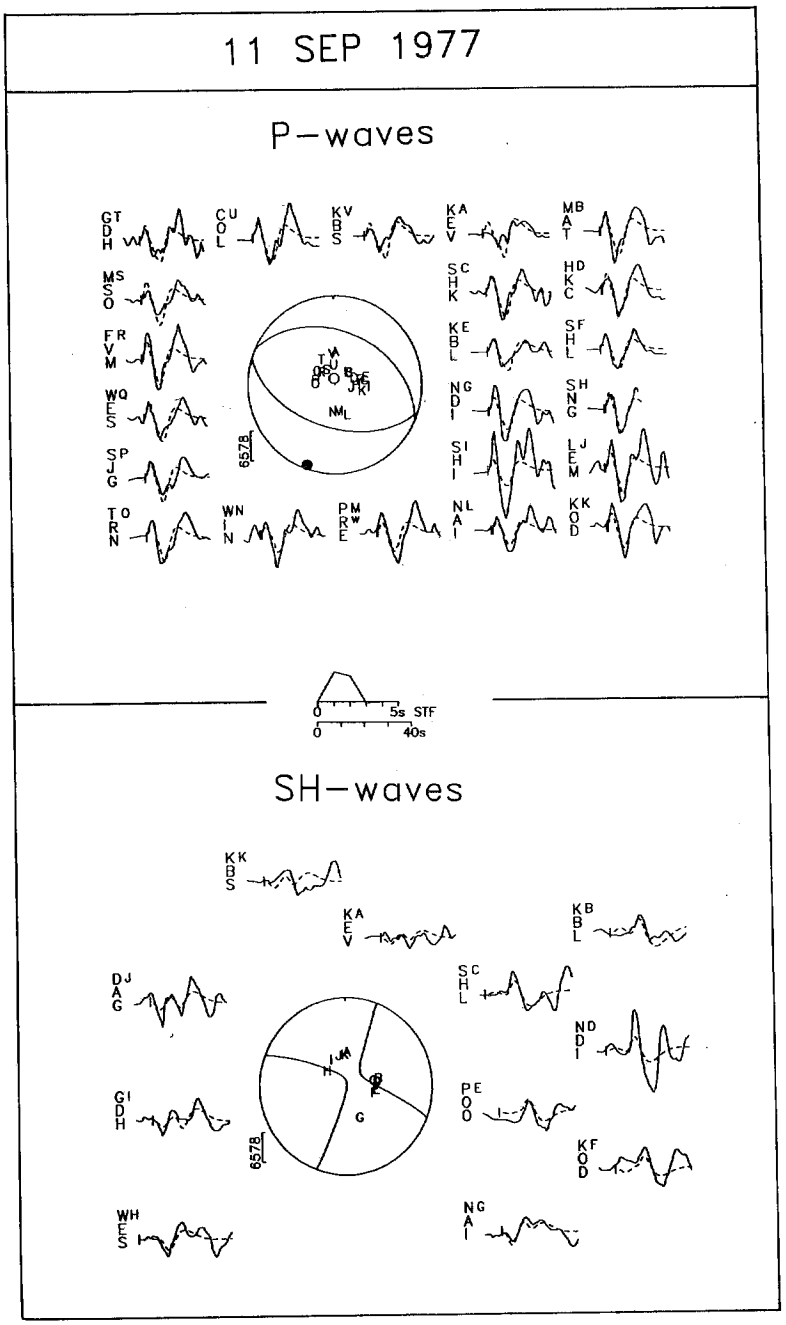


Fig. 8 — Observed (solid) and synthetic (dashed) long-period seismograms for the September 11, 1977 earthquake. All symbols are as described in Fig. 2.

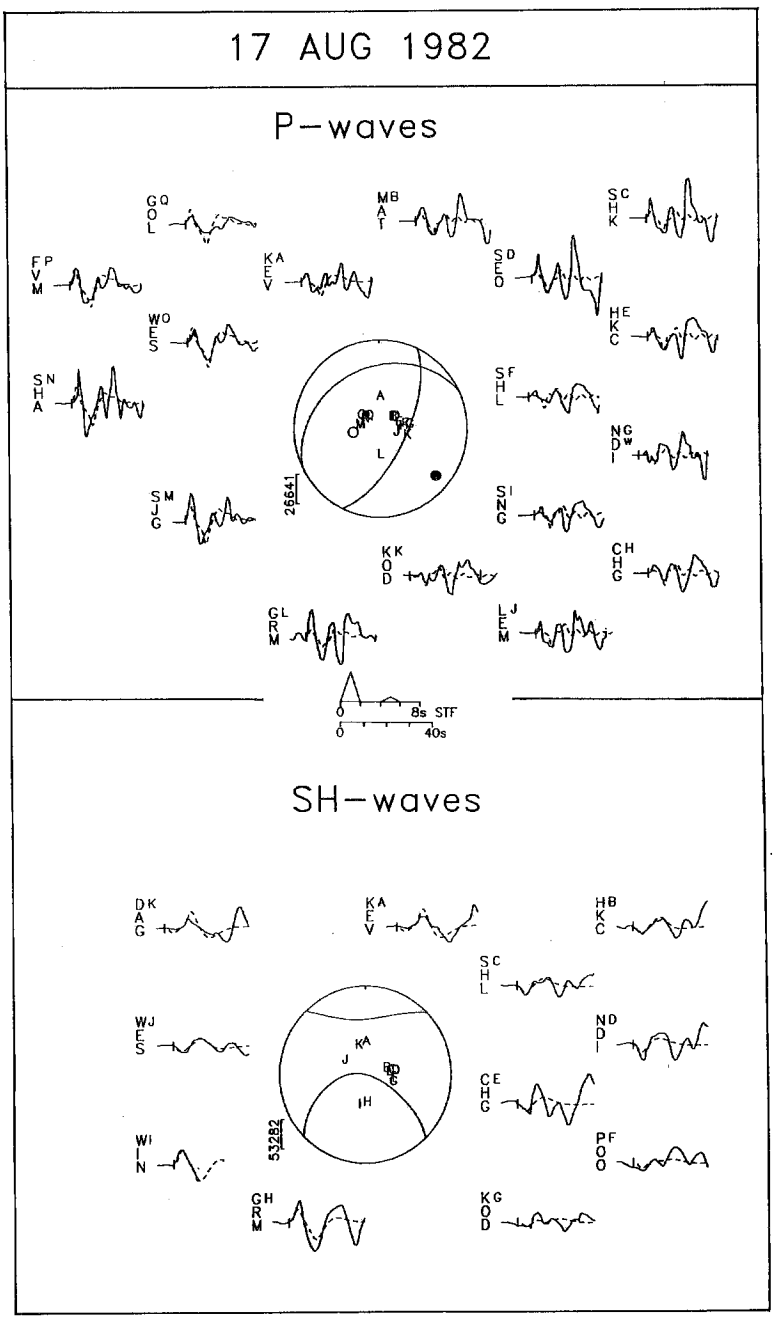


Fig. 9 — Observed (solid) and synthetic (dashed) long-period seismograms for the August 17, 1982 earthquake. All symbols are as described in Fig. 2.

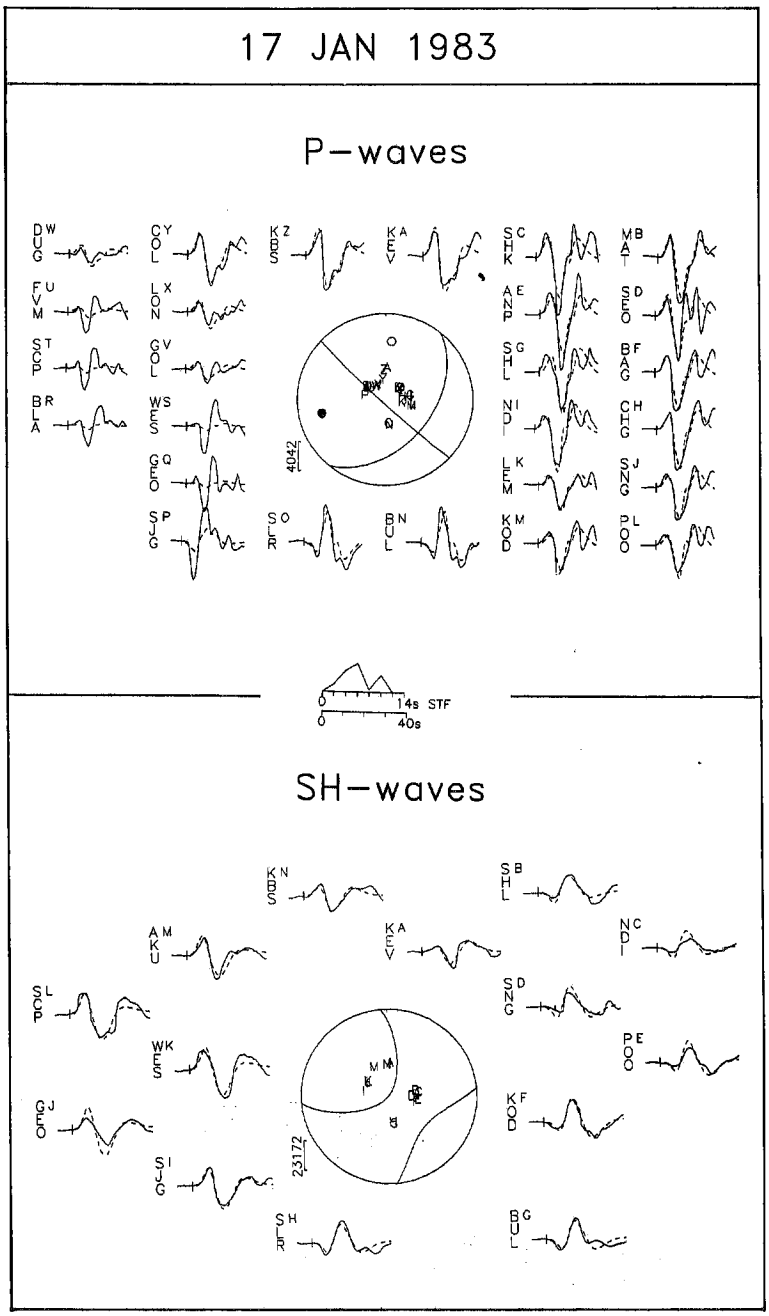


Fig. 10 — Observed (solid) and synthetic (dashed) long-period seismograms for the January 17, 1983 earthquake. All symbols are as described in Fig. 2.

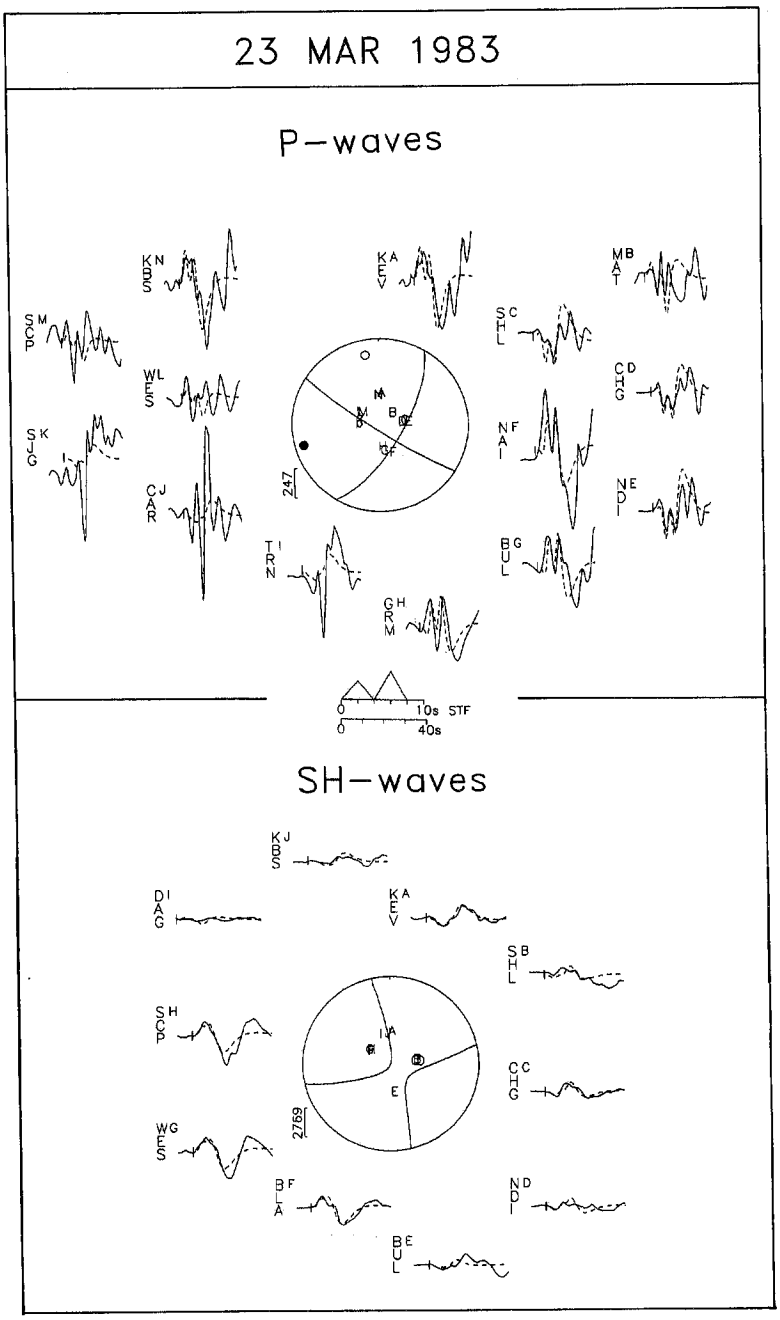


Fig. 11 — Observed (solid) and synthetic (dashed) long-period seismograms for the March 23, 1983 earthquake. All symbols are as described in Fig. 2.

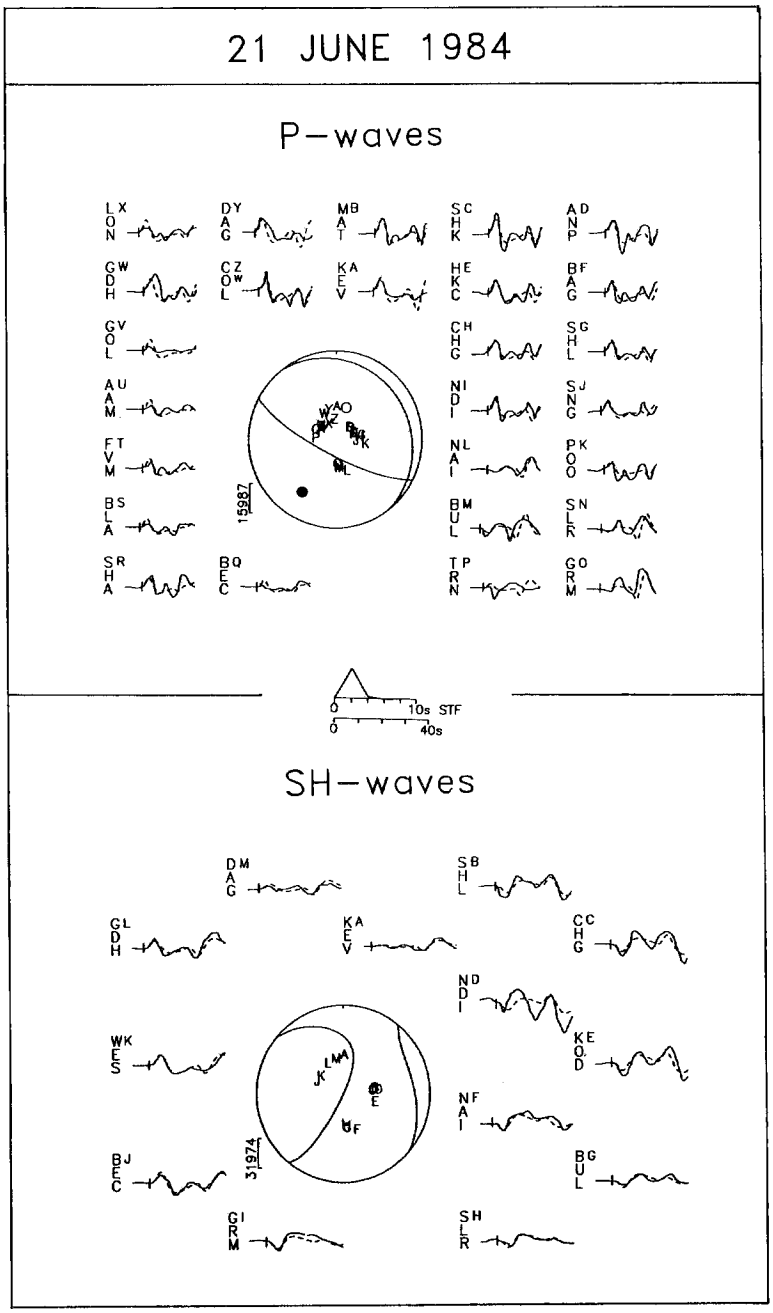


Fig. 12 — Observed (solid) and synthetic (dashed) long-period seismograms for the June 24, 1984 earthquake. All symbols are as described in Fig. 2.

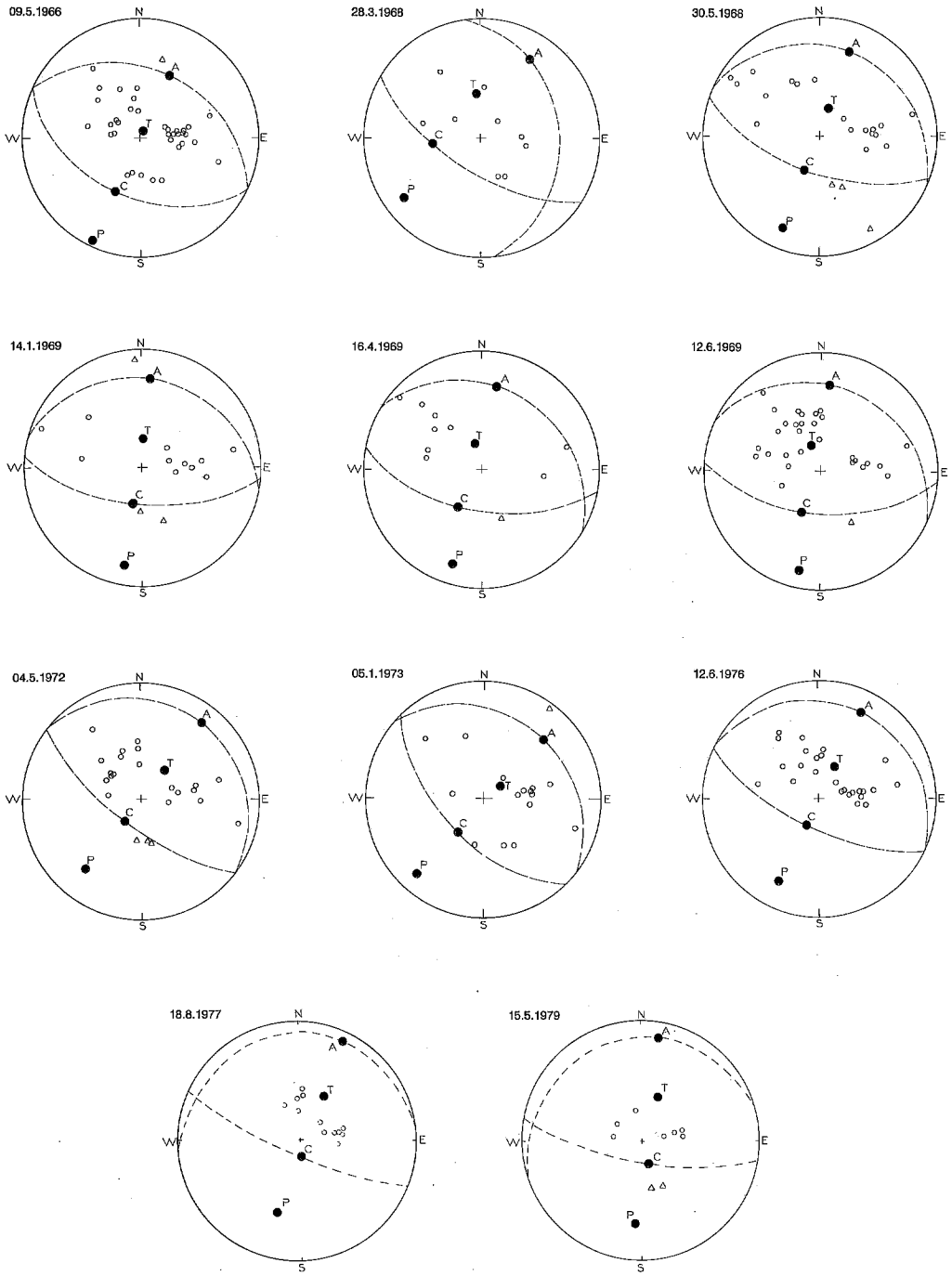


Fig. 13 — Fault plane solutions of the 11 additional events used, based on first motion polarity data (after Papadimitriou et al., 1991). The date of each event is noted on the top of each sphere.

**Table 2 — The parameters of the focal mechanism of the shallow earthquakes which occurred along the Hellenic arc during the period 1959-1985.**

| | Date | Origin Time | Epicentral Coordinates φ°N | λ°E | h (km) | $M_s$ | P | | T | | Nodal Plane 1 strike° | dip° | rake° | Nodal Plane 2 strike° | dip° | rake° | Ref. |
|---|---|---|---|---|---|---|---|---|---|---|---|---|---|---|---|---|---|
| 1 | 1959, Nov. 15 | 17:08:43 | 37.8 | 20.5 | 12 | 6.8 | 254 | 38 | 12 | 31 | 46 | 37 | 187 | 311 | 86 | 307 | 1 |
| 2 | 1963, Dec. 16 | 13:47:53 | 37.0 | 21.0 | 17 | 5.9 | 197 | 29 | 11 | 61 | 296 | 16 | 101 | 105 | 74 | 87 | 1 |
| 3 | 1966, May 09 | 00:42:53 | 34.4 | 26.4 | 16 | 5.8 | 205 | 05 | 25 | 85 | 295 | 40 | 90 | 115 | 50 | 90 | 2 |
| 4 | 1968, Mar. 28 | 07:39:59 | 37.8 | 20.9 | 6 | 5.9 | 231 | 20 | 355 | 59 | 354 | 34 | 137 | 122 | 67 | 63 | 3 |
| 5 | 1968, May 30 | 17:40:26 | 35.4 | 27.9 | n | 5.9 | 202 | 20 | 18 | 70 | 293 | 25 | 90 | 110 | 76 | 90 | 2 |
| 6 | 1969, Jan. 14 | 23:12:06 | 36.1 | 29.2 | n | 6.2 | 190 | 18 | 05 | 70 | 282 | 25 | 95 | 95 | 75 | 87 | 2 |
| 7 | 1969, Apr. 16 | 23:21:06 | 35.2 | 27.7 | 35 | 5.5 | 197 | 16 | 347 | 71 | 301 | 30 | 109 | 100 | 60 | 80 | 2 |
| 8 | 1969, Jun. 12 | 15:13:31 | 34.4 | 25.0 | 19 | 6.1 | 192 | 17 | 340 | 72 | 294 | 29 | 105 | 95 | 61 | 80 | 2 |
| 9 | 1969, Jul. 08 | 08:09:13 | 37.5 | 20.3 | 12 | 5.9 | 242 | 28 | 44 | 60 | 353 | 18 | 116 | 146 | 74 | 82 | 1 |
| 10 | 1972, May 04 | 21:39:57 | 35.1 | 23.6 | 40 | 6.5 | 219 | 27 | 39 | 63 | 308 | 18 | 90 | 129 | 72 | 90 | 4 |
| 11 | 1972, Sep. 17 | 14:07:15 | 38.3 | 20.3 | 8 | 6.3 | 267 | 20 | 01 | 11 | 45 | 68 | 186 | 313 | 84 | 158 | 1 |
| 12 | 1973, Jan. 05 | 05:49:18 | 35.8 | 21.9 | n | 5.6 | 218 | 15 | 46 | 74 | 306 | 30 | 82 | 136 | 60 | 93 | 5 |
| 13 | 1973, Nov. 29 | 10:57:44 | 35.2 | 23.8 | 22 | 6.0 | 188 | 07 | 337 | 82 | 283 | 38 | 97 | 94 | 52 | 85 | 1 |
| 14 | 1976, May 11 | 16:59:45 | 37.4 | 20.4 | 16 | 6.5 | 232 | 31 | 44 | 59 | 335 | 14 | 106 | 139 | 76 | 86 | 1 |
| 15 | 1976, Jun. 12 | 00:59:18 | 37.5 | 20.6 | 8 | 5.8 | 206 | 25 | 26 | 65 | 297 | 20 | 90 | 117 | 70 | 90 | 6 |
| 16 | 1977, Aug. 18 | 09:27:41 | 35.3 | 23.5 | 38 | 5.6 | 197 | 44 | 29 | 56 | 270 | 12 | 62 | 114 | 79 | 96 | 6 |
| 17 | 1977, Sep. 11 | 23:19:19 | 34.9 | 23.0 | 16 | 6.3 | 201 | 05 | 351 | 84 | 295 | 40 | 95 | 109 | 50 | 86 | 1 |
| 18 | 1979, May 15 | 06:59:23 | 34.6 | 24.5 | 35 | 5.7 | 184 | 29 | 16 | 59 | 253 | 17 | 65 | 100 | 75 | 97 | 6 |
| 19 | 1982, Aug. 17 | 22:22:20 | 33.7 | 22.9 | 15 | 6.4 | 147 | 14 | 259 | 56 | 246 | 31 | 125 | 26 | 65 | 71 | 1 |
| 20 | 1983, Jan. 17 | 12:41:30 | 38.1 | 20.2 | 11 | 7.0 | 257 | 27 | 06 | 33 | 39 | 45 | 175 | 132 | 87 | 45 | 1 |
| 21 | 1983, Mar. 23 | 23:51:05 | 38.2 | 20.3 | 7 | 6.2 | 255 | 11 | 349 | 19 | 31 | 69 | 174 | 123 | 84 | 21 | 1 |
| 22 | 1984, Jun. 21 | 10:43:46 | 35.4 | 23.3 | 40 | 6.2 | 213 | 30 | 18 | 59 | 322 | 16 | 114 | 117 | 75 | 83 | 1 |
| 23 | 1985, Apr. 21 | 08:49:42 | 35.7 | 22.2 | 35 | 5.6 | 193 | 10 | 60 | 75 | 269 | 36 | 71 | 112 | 56 | 103 | 7 |

1. This study, 2. McKenzie (1972), 3. Anderson and Jackson (1987), 4. Kiratzi and Langston (1989), 5. McKenzie (1978), 6. Taymaz et al. (1990), 7. NEIS.

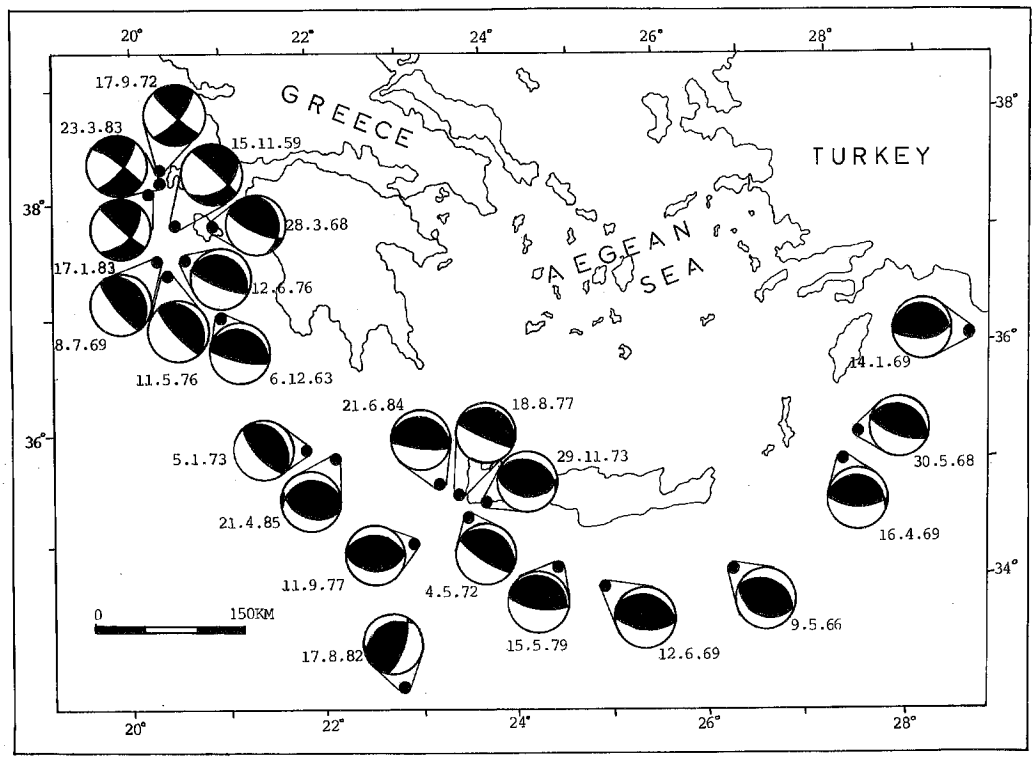


Fig. 14 — Epicentres and fault plane solutions of the earthquakes listed in Table 2. Compressional quadrants are solid. The date of each event is also noted.

confirm the above solution. The best fit P wave solution gives a centroid depth of 7 km. The seismic moment is $1.9*10^{25}$ dyn cm and the duration of the source time function is about 8 s. The Harvard centroid moment tensor (HMCT) solution for this event is also a strike slip mechanism with a depth of 33 km (Dziewonski et al., 1983).

*June 21, 1984.* This event occurred in the sea near the west coast of Crete. Many P and S wave records were available for this earthquake, resulting in a very good station coverage for both P and SH waves (Fig. 12). A good overall fit to the observed waveforms is obtained with a centroid depth of 40 km and a thrust-faulting mechanism (322/16/114) with the fault plane trending SW-NE and dipping NE. The seismic moment is $1.3*10^{25}$ dyn cm and the total duration of the rupture is about 4 s. The P waveforms which have dilatational first motion, that is, at stations NAI, BUL, SLR and GRM, and those with almost nodal first motion (TRN and BEC), contributed in fixing the strike of the solution. For the SH waveforms, there are many stations displaying clear compressional first motions, and the same for dilatational first motions, as well as one clear nodal (KEV). The very good matching of the synthetic to the observed SH waveforms confirms the solution stability.

Solutions for this event have been suggested by Papadimitriou (1988), Ioannidou (1989) and Taymaz et al. (1990). From all these, the last is similar to the one suggested here.

## ADDITIONAL FAULT PLANE SOLUTIONS

In addition to the eleven events analyzed above, fault plane solutions for 12 other earthquakes are used here in order to have a more global image of the tectonic processes of the area under study. All these solutions are taken from the study of Papazachos et al. (1991) and Papadimitriou et al. (1991). These authors had collected all the available and reliable data and solutions based both on first onsets of long-period P waveforms and waveform analysis.

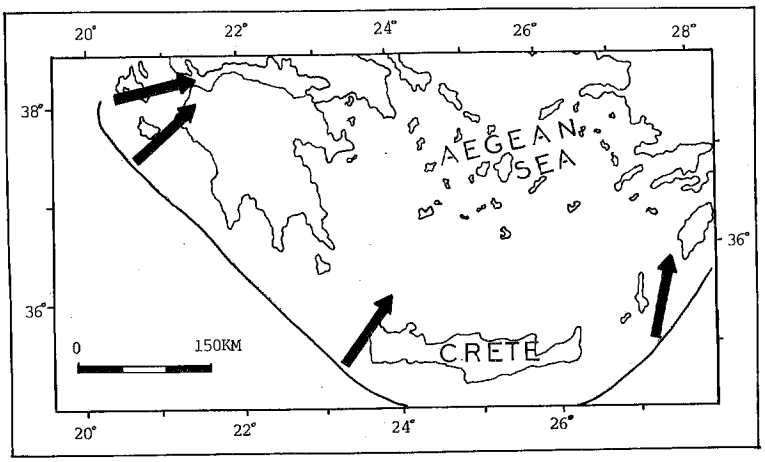


Fig. 15 — The direction of the axis of maximum compression P along the Hellenic Arc.

Some of these solutions were accepted as they were published in previous studies and some of them were redetermined by the authors.

Fig. 13 illustrates the fault plane solutions of these events and the data on which they are based, except for the April 21, 1985 event, the solution of which is taken from NEIS. Table 2 gives information on the source parameters of all the events considered in this study; that is, the date of occurrence, the origin time, the epicentral coordinates, the surface wave magnitude, the focal depth in km, the azimuth and plunge of the maximum compressional P, and the maximum tensional T, axes, the strike, dip and rake of the two nodal planes and finally the references from which they have been taken.

## REPRESENTATIVE FAULT PLANE SOLUTIONS

All the fault plane solutions mentioned above, for a total of 23 earthquakes, are shown in Fig. 14. The whole set was separated into four groups, on the basis of the type of faulting, the spatial distribution of the earthquake epicenters and seismicity criteria (Papazachos, 1990). The first group contains the four earthquakes which occurred near Cephalonia and are characterized by strike-slip faulting. The second group contains the events which occurred near Zakynthos, and the third and fourth groups the events which occurred in the western and eastern part of Crete, respectively. The events of the last three groups exhibit dip-slip thrust faulting.

For each one of these groups the *representative* focal mechanism tensor **F** was determined on the basis of a formal technique introduced by Papazachos and Kiratzi (1992). The above authors, based on previous work by Kostrov (1974) and Jackson and McKenzie (1988), propose the following formula for the determination of **F**:

$$\boldsymbol{F}=\frac{\sum_{n=1}^{N} M_o^n F^n}{\sum_{n=1}^{n} M_o^n}, \tag{1}$$

where $M_o$ is the scalar moment of the $n$th earthquake, and

$$\boldsymbol{F}^n=\boldsymbol{u}.\boldsymbol{n}+\boldsymbol{n}.\boldsymbol{u}, \tag{2}$$

where $\boldsymbol{u}$ and $\boldsymbol{n}$ are unit vectors parallel to the slip vector and normal to the fault plane, respectively. $F^n$ is a function of the strike $\phi$, of the dip $\delta$, and of the rake $\lambda$, of the earthquake (Aki and Richards, 1980). If the *representative* focal mechanism tensor is multiplied by the scalar moment rate $\dot{M}_o$, for each region, then we get the region's moment rate tensor $\dot{M}$.

By this technique, we can group broad seismic regions where faulting (strike, slip, rake) does not vary considerably, and calculate **F** for each belt from eqn. (1). In this case, $N$ is the number of earthquakes of each belt for which reliable solutions are available, regardless of the time in which they occurred or the completeness of the data. Thus, the number of fault plane solutions used for the determination of **F** for each zone is increased. The components of this tensor and its eigensystem, which corresponds to the P, T and null-axes, is calculated for each group of events.

*Group 1 (Cephalonia island).* This first group contains the four strike-slip events which occurred near Cephalonia (numbered 1, 11, 20 and 21 in Table 2). The components of the **F** tensor in the coordinate system used (1:North, 2:East, 3:Down) for this region are:

| | | |
|---|---|---|
| *.68* | *-.09* | *.53* |
| *-.09* | *-.67* | *.46* |
| *.53* | *.46* | *-.53* |

and its eigenvectors are:

| | *P* | *T* | *B* |
|---|---|---|---|
| $\lambda_F$ | *-.98* | *.98* | *-.004* |
| *Azimuth(°)* | *76* | *6* | *131* |
| *Plunge(°)* | *-30* | *30* | *44* |

It is seen that the axis of maximum compression has a mean azimuth of 76°, dipping with an angle of 30° to the Mediterranean, and the axis of maximum tension with a mean azimuth of 6° has the same plunge (30°) dipping NE.

*Group 2 (Zakynthos island).* Five events which are located near Zakynthos are included in this second group (numbered 2, 4, 9, 14 and 15 in Table 2). All of them have dip-slip thrust mechanisms. The components of the **F** tensor in the coordinate system used are:

| | | |
|---|---|---|
| *-.16* | *-.24* | *.61* |
| *-.24* | *-.34* | *.57* |
| *.61* | *.57* | *.49* |

and its eigenvectors are:

| | *P* | *T* | *B* |
|---|---|---|---|
| $\lambda_F$ | *-.97* | *.97* | *-.003* |
| *Azimuth(°)* | *49* | *37* | *136* |
| *Plunge(°)* | *-30* | *60* | *5* |

This means that the axis of maximum compression has a mean azimuth 49°, dipping at an angle of 30° to the Mediterranean, while the axis of maximum tension has a mean azimuth of 37°, dipping at an angle of 60° to the NE.

*Group 3 (West Crete).* This group includes eight events which occurred west and southwest of Crete exhibiting dip-slip thrust mechanisms (numbered 10, 12, 13, 16, 17, 18, 22 and 23 in Table 2). The components of the **F** tensor in the coordinate system used are:

| | | |
|---|---|---|
| *-.46* | *-.26* | *.60* |
| *-.26* | *-.18* | *.36* |
| *.60* | *.36* | *.63* |

and its eigenvectors are:

| | P | T | B |
|---|---|---|---|
| $\lambda_F$ | -.92 | .94 | -.02 |
| Azimuth(°) | 31 | 31 | 121 |
| Plunge(°) | -24 | 66 | 0 |

It is observed that the axis of maximum compression has a mean azimuth of 31°, dipping at an angle of 24° to the Mediterranean, and the axis of maximum tension, with an azimuth of 31°, dips at an angle of 66° to NE.

*Group 4 (East Crete).* Five events which occurred south and east of Crete are considered here (numbered 3, 5, 6, 7and 8 in Table 2). The components of the **F** tensor for this region and in the coordinate system used are:

| | | |
|---|---|---|
| -.74 | -.20 | .58 |
| -.20 | -.05 | -.07 |
| .58 | -.07 | .80 |

and its eigenvectors are:

| | P | T | B |
|---|---|---|---|
| $\lambda_F$ | -.98 | 0.99 | -.006 |
| Azimuth(°) | 13 | 0 | 102 |
| Plunge(°) | -18 | 72 | 4 |

It is observed that the axis of maximum compression in this region has a mean azimuth 13°, dipping at an angle of 18° to the Mediterranean. The axis of maximum tension has a plunge of 72° with a purely north direction.

## SUMMARY AND CONCLUSIONS

Long- and short- period teleseismically recorded body waves have been used to determine the source mechanism, centroid depth and source time function of seven large earthquakes which occurred in the Ionian islands during the last 30 years, and four events which occurred near Crete during the last 20 years.

The source mechanisms obtained for the four earthquakes, of which the epicenters are located west of Cephalonia and northwest of Zakynthos islands, are of right-lateral strike-slip type, with depths ranging between 7 and 12 km. Their planes strike from SW to NE and dip to the SE. The mechanisms of the 1959 and 1972 earthquakes show a small normal component, while the other two a small thrust component. All have the same slip direction from SW to NE.

The source characteristics of the seven earthquakes located west and southwest of Zakynthos and west and southwest of Crete, are of the same type. All show thrust faulting with nearly pure dip-slip motion. The fault planes of the events which occurred near Zakynthos, have almost the same strike (NW-SE) parallel to the axis of the Hellenic Arc in this region. The slip direction is almost SW-NE and the horizontal projections of the slip vector is parallel to the direction of relative plate motion.

The three events which occurred near the southwestern coasts of Crete, have fault planes striking E-W, with the axes of maximum compression nearly horizontal and azimuth ranging from 180° to 220°. It is interesting to note that going from Zakynthos to Crete, the slip direction changes slightly to the north. The focal mechanism of the August 17, 1982 event exhibited a different mechanism, with the axis of maximum compression P having an azimuth of 147° and a plunge of 14°, resulting in an almost SSE-NNW compression there.

Summarizing, it can be said that the thrust zone due to subduction in the southern Aegean terminates near Zakynthos island. In Cephalonia, strike-slip dextral faulting is observed which can be explained by accepting the suggestion of a transform fault in the area, which connects the thrust zone of the Hellenic Arc in the south, with the thrust zone of the Apulian plate in the north. From Zakynthos to Crete, the motion is purely compressional, with a direction almost NE. These results are in good agreement with a global seismotectonic study of the Aegean area by Papazachos et al. (1986, 1991).

The calculation of the *representative* focal mechanism tensor **F** provided the azimuth and the dip of the axis of maximum compression P, and the axis of maximum tension T, along the Hellenic Arc. This P axis is plotted in the mean epicenter of each group in Fig. 15. It is seen that this orientation is not stable but the values of both its direction and dip decrease going from southwest to east. It is observed that this axis has an azimuth of 76° and a plunge of 30° in the northwestern termination of the Arc, in Cephalonia. Near Zakynthos, the value of the azimuth becomes smaller, that is, 49°, while the plunge remains the same (30°). In the area of western Crete, both values changed to 31° and 24° for azimuth and plunge, respectively, while in the eastern part of Crete the azimuth is even smaller, 13°, and the same for the plunge (18°). This is in good agreement with LePichon and Angelier (1979) who suggested that there is a 30° clockwise rotation of Peloponnesus and western Crete, and that this rotation progressively changes to counterclockwise to the east of Crete. They also found that the dips of the sinking slab are different along the arc, and decrease from west to east.

Another result that is interesting to note is that the extension along the Arc has a plunge between 30° and 72°. These values are much larger than the angle of the subduction, which is found to be 23° in the upper part of the descending slab, and 38° for its steeper part (Papazachos et al., 1991). This supports the suggestion made by Papazachos (1977, 1990) according to which the T axis does not follow the dip direction of the Benioff zone, but dips steeper.

**Acknowledgements.** The author would like to express her sincere appreciation to Prof. B.C. Papazachos for the critical reading of the manuscript, his constructive ideas and his suggestions. Thanks are also given to Dr. H. Lyon-Caen for her helpful suggestions and discussions, and to C.B. Papazachos who kindly provided his assistance and computer program. The comments of the two anonymous reviewers are very much appreciated.

## REFERENCES


Aki K. and Richards P.G.; 1980: *Quantitative Seismology: Theory and Methods.* Vol. I W.H Freeman, S. Fransisco, 557 pp.

Anderson H. and Jackson J.; 1987: *Active tectonics of the Adriatic region.* Geophys. J. R. astr. Soc., **91**, 937-983.

Beisser M., Wyss M. and Kind R.; 1990: *Inversion of source parameters for subcrustal earthquakes in the Hellenic Arc.* Geophys. J. Int., **103**, 439-450.

Bezzeghoud M.; 1987: *Inversion et analyse spectrale des ondes P.* These de Doctorat de l'Universite Paris VII, 232 pp.

Brirish Petroleum; 1971: *The geological results of petroleum exploration in western Greece.* Institute for Geology and Subsurface Research, Athens, No. 10.

Dewey J.F. and Sengor C.; 1979: *Aegean and surrounding region: Complex multiplate and continuum tectonics in a convergent zone.* Bull. Geol. Soc. Am., **90**, 84-92.

Dziewonski A.M., Friedman A. and Woodhouse J.H.; 1983: *Centroid-moment tensor solutions for January-March, 1983.* Phys. Earth. Plan. Int., **33**, 71-75.

Finetti I.; 1976: *Mediterranean ridge: A young submerged chain associated with the Hellenic Arc.* Boll. Geof. Teor. Appl., **19**, 31-65.

Ioannidou E.; 1989: *Charecteristic parameters of seismic source by the method of body wave inversion: Greece and the surrounding area.* Ph. D. Thesis, Athens University, 282 pp.

Jackson J. and McKenzie D.; 1988: *The relationship between plate motions and seismic moment tensors, and the rates of active deformation in the Mediterranean and Middle East.* Geophys. J., **93**, 45-73.

Kiratzi A.A. and Langston C.; 1989: *Estimation of earthquake source parameters of the May 4, 1972 event of the Hellenic Arc by the inversion of waveform data.* Phys. Earth Planet. Interiors, **57**, 225-232.

Kiratzi A.A. and Langston C.; 1991: *Moment tensor inversion of the January 17, 1983 Kefallinia event of Ionian Islands (Greece).* Geophys. J. Int., **105**, 529-535.

Kostrov, V.; 1974: *Seismic moment and energy of earthquakes, and seismic flow of rock.* Izv. Acd. Sci. USSR Phys. Solid Earth, **1**, 23-44.

LePichon X. and Angelier J.; 1979: *The Hellenic Arc and Trench system: a key to the neotectonic evolution of the eastern Mediterranean area.* Tectonophysics, **60**, 1-42.

Liakopoulou F., Pearce R.G. and Main I.G.; 1991: *Source mechanisms of recent earthquakes in the Hellenic arc from broadband data.* Tectonophysics, **200**, 233-248.

McCaffrey, R. and Abers, G.; 1988: *SYN3: A program for inversion of teleseismic body waveform on microcomputers.* Scientific Report No. 1, AFGL-TR-880099.

McKenzie D.P.; 1972: *Active tectonics in the Mediterranean region.* Geophys. J. R. astr. Soc., **30**, 109-185.

McKenzie D.P.; 1978: *Active tectonics of the Alpine-Himalayan belt: the Aegean sea and surrounding region.* Geophys. J. R. astr. Soc., **55**, 217-254.

Nabelek J.; 1984: *Determination of earthquake source parameters from inversion of body waves.* Ph. D. Dissertation, Macha-ssusetts Institute of Technology, 360 pp.

Nabelek J.; 1985: *Geometry and mechanism of faulting of the 1980 El Asnam, Algeria earthquake from inversion of teleseismic body waves and comparison with field observations.* J. Geophys. Res., **90**, 12713-12728.

North R.G.; 1977: *Seismic moment, source dimensions, and stresses associated with earthquakes in the Mediterranean and Middle East.* Geoph. J. R. astr. Soc., **48**, 137- 161.

Panagiotopoulos D.G. and Papazachos B.C.; 1985: *Travel times of Pn waves in the Aegean and surrounding area.* Geoph. J. R. astr. Soc., **80**, 165-176.

Papadimitriou E.E. and Papazachos B.C.; 1985: *Evidence for premonitory patterns in the Ionian islands (Greece).* Earthq. Pred. Res., **3**, 95-103.

Papadimitriou E.E., Kiratzi A.A. and Papazachos B.C.; 1991: *Fault plane solutions of strong earthquakes in the Aegean and surrounding area.* Publ. Geophys. Lab., Univ. Thessaloniki, **5**, 75 pp.

Papadimitriou P.; 1988: *Etude de la structure du manteau superieur de l'Europe et modelisation des ondes de volume engendres par les seismes Egeens.* These de Doctorat de l' Universite Paris VII, 211 pp.

Papazachos, B.C.; 1990: *A lithospheric model to interprete focal properties of intermediate and shallow shocks in central Greece.* Pure Appl. Geophys., **115**, 655-666.

Papazachos, B.C.; 1990: *Seismicity of the Aegean and surrounding area.* Tectonophysics, **178**, 287-308.

Papazachos B.C. and Comninakis P.E.; 1969: *Geophysical features of the Greek island arc and eastern Mediterranean ridge.* C. R. Conference Reunie a Madrid, **16**, 74-75.

Papazachos B.C. and Comninakis P.E.; 1971: *Geophysical and tectonic features of the Aegean Arc.* J. Geophys. Res., **76**, 8517-8533.

Papazachos B.C., Kiratzi A.A., Hatzidimitriou P.M. and Rocca A.Ch.; 1984: *Seismic faults in the Aegean area.* Tectonophysics, **106**, 71-85.

Papazachos B.C., Kiratzi A.A., Hatzidimitriou P.M. and Karacostas B.G.; 1986: *Seismotectonic properties of the Aegean area that restrict valid geodynamic models.* In: 2nd Wegener Conf., Dionysos, Greece, 14-16 May 1986, pp. 1-16.

Papazachos B.C., Kiratzi A.A. and Papadimitriou E.E.; 1991: *Regional focal mechanisms for earthquakes in the*

*Aegean area*. Pure Appl. Geophys., **136**, 405-420.

Papazachos C.B. and Kiratzi A.A.; 1992: *A formulation for reliable estimation of active crustal deformation and its application to central Greece*. Geophys. J. Int., **111**, 424-432.

Scordilis E.M., Karakaisis G.F., Karacostas B.G., Panagiotopoulos D.G., Comninakis P.E. and Papazachos B.C.; 1985: *Evidence for transform faulting in the Ionian sea: The Cephalonia island earthquake sequence of 1983*. Pure Appl. Geophys., **123**, 388-397.

Stride A.H., Belderson R.H. and Kenyon N.H.; 1977: *Evolving Miogeanticlines of the Eastern Mediterranean (Hellenic, Calabrian and Cyprus outer ridges)*. Phil. Trans. R. Soc. Lond. A, **284**, 255.

Taymaz T., Jackson J. and Westaway R.; 1990: *Earthquake mechanisms in the Hellenic Trench near Crete*. Geophys. J. Int., **102**, 695-731.